

Plastic CTOD as fatigue crack growth characterising parameter in 2024-T3 and 7050-T6 aluminium alloys using DIC

Journal:	<i>Fatigue & Fracture of Engineering Materials & Structures</i>
Manuscript ID	FFEMS-8475.R1
Manuscript Type:	Special Issue: Characterisation of Crack Tip Fields 5
Date Submitted by the Author:	n/a
Complete List of Authors:	Vasco-Olmo, Jose; Universidad de Jaen, Mechanical Engineering Diaz, Francisco; Universidad de Jaen, Mechanical Engineering Antunes, Fernando; University of Coimbra, Department of Mechanical Engineering James, Neil; University of Plymouth, School of Marine Sciences & Engineering

SCHOLARONE™
Manuscripts

J.M. Vasco-Olmo*, F.A. Díaz, F.V. Antunes, M.N. James. Plastic CTOD as fatigue crack growth characterising parameter in 2024-T3 and 7050-T6 aluminium alloys using DIC. *Fatigue & Fracture of Engineering Materials & Structures*, 43: 1719–1730, 2020. T1, Q2 (37/133 en Mechanical Engineering, IF 2020: 3.459). <https://onlinelibrary.wiley.com/doi/full/10.1111/ffe.13210>.

Plastic CTOD as fatigue crack growth characterising parameter in 2024-T3 and 7050-T6 aluminium alloys using DIC

J.M. Vasco-Olmo^{1*}, F.A. Díaz¹, F.V. Antunes², M.N. James^{3, 4}

¹ Departamento de Ingeniería Mecánica y Minera, University of Jaén, Jaén, Spain.

² Department of Mechanical Engineering, University of Coimbra, Coimbra, Portugal.

³ School of Engineering, University of Plymouth, Plymouth, United Kingdom.

⁴ Department of Mechanical Engineering, Nelson Mandela Metropolitan University, Port Elisabeth, South Africa.

*corresponding author: jvasco@ujaen.es

Abstract. The plastic range of crack tip opening displacement (CTOD) has been used for the experimental characterisation of fatigue crack growth for 2024-T3 and 7050-T6 aluminium alloys using digital image correlation (DIC). Analysis of a complete loading cycle allowed resolving the CTOD into elastic and plastic components. Fatigue tests were conducted on compact-tension (CT) specimens with a thickness of 1 mm and a width of 20 mm at stress ratios of 0.1, 0.3 and 0.5. The range of plastic CTOD could be related linearly to da/dN independent of stress ratio for both alloys. To facilitate accurate measurements of CTOD, a method was developed for correctly locating the crack tip and a sensitivity analysis was performed to explore the effect of measurement position behind the crack tip on the CTOD. The plastic range of CTOD was demonstrated to be a suitable alternate parameter to the stress intensity factor range for characterising fatigue crack propagation. A particularly innovative aspect of the work is that the paper describes a DIC-based technique that the authors believe gives a reliable way to determine the appropriate position to measure CTOD.

Keywords. CTOD, fatigue crack growth, DIC, 2024-T3 and 7050-T6 aluminium alloys.

Nomenclature:

1		
2		
3		
4		
5	a:	crack length
6		
7	CJP:	crack tip fields model developed by Christopher, James and Patterson
8		
9	COD:	crack opening displacement
10		
11	CT:	compact tension specimen
12		
13	CTOD:	crack tip opening displacement
14		
15	CTOD_{el}:	elastic component of crack tip opening displacement
16		
17	CTOD_p:	plastic component of crack tip opening displacement
18		
19	CTOD_t:	total crack tip opening displacement
20		
21	da/dN:	crack growth rate per cycle
22		
23	DIC:	digital image correlation technique
24		
25	E:	Young's modulus
26		
27	L_x:	distance in the parallel direction to the crack for the CTOD measurement
28		
29	L_y:	distance in the perpendicular direction to the crack plane for the CTOD measurement
30		
31		
32		
33	MT:	middle tension specimen
34		
35	P:	load
36		
37	R:	ratio between the minimum and maximum load
38		
39	W:	width of the specimen
40		
41	ΔCOD:	range of crack opening displacement
42		
43	ΔCTOD:	range of crack tip opening displacement
44		
45	ΔCTOD_{el}:	range of elastic crack tip opening displacement
46		
47	ΔCTOD_p:	range of plastic crack tip opening displacement
48		
49	ΔJ:	range of <i>J</i> integral
50		
51	ΔK:	range of stress intensity factor
52		
53	ν:	Poisson's ratio of the material
54		
55	σ_{ys}:	yield stress of the material
56		
57		
58		
59		
60		

1. Introduction

Although composite materials are currently being extensively used in modern commercial aircraft, aluminium alloys (AA) remain the materials of choice for the airframe. Among them, AA2024-T3 and AA7050-T6 are particularly relevant to the aerospace industry due to their high strength and good resistance to fatigue crack propagation and corrosion¹. Characterising fatigue crack growth rate using CTOD has been the subject of a significant body of research, but the ability of DIC measurements to obtain the plastic range of CTOD (ΔCTOD_p) is still somewhat controversial. The present authors have previously presented a preliminary study of fatigue crack growth in commercially pure titanium and identified a 2D DIC technique that allows accurate identification of the plastic range of CTOD². A linear relationship was observed between crack propagation rate (da/dN) and ΔCTOD_p . This work extends the technique to the characterisation of fatigue crack propagation in two aluminium alloys commonly used in aircraft industrial applications.

The stress intensity factor range (ΔK) has traditionally been used as a characterising parameter for fatigue crack growth rate in applications subjected to small-scale yielding using the Paris relationship^{3,4}. However, this relationship has some limitations^{5,6}: (i) it is based on empirical observations and does not add understanding on the mechanisms driving fatigue crack growth, and the constants obtained from the fitting process contain physically unjustifiable units; (ii) it is only valid for (relatively) large cracks under small-scale yielding conditions subjected to constant amplitude loading cycle; and (iii) crack growth rate per cycle depends on other parameters such as applied load ratio and load history which can invalidate the similitude concept that underpins the limited validity of the Paris power relationship.

These limitations reflect the fact that stress intensity factor was a parameter defined to describe linear elastic conditions at the crack tip, while fatigue crack propagation is controlled by nonlinear plasticity processes at the crack tip. The two most frequently used parameters in elastic-plastic fracture mechanics are CTOD and the J -contour integral⁷. While both parameters are applied to materials that exhibit elastic-plastic behaviour at the crack tip and can also be used as a fracture criterion, the J -integral is a global nonlinear elastic parameter and hence can also suffer from plasticity-induced loss of similitude. CTOD is a local parameter used to measure the opening originated at the tip of a crack as the component is loaded that therefore takes account of crack tip plasticity, although defining the precise point behind the absolute crack tip where the opening displacement should be characterised can also be problematic. CTOD is used in this work as the parameter for characterising fatigue crack growth and a DIC-based

1
2
3 technique is described that the authors believe gives a reliable way to find the
4 appropriate point to measure CTOD.
5

6 Since Wells⁸ proposed CTOD in 1961, it has been extensively used for fatigue crack
7 growth characterisation since it is a more mechanistically-based approach⁶ than the
8 purely phenomenological Paris relationship. It is also the case that the plastic range of
9 CTOD includes effects of crack shielding, residual stresses and fatigue threshold in an
10 intrinsic way⁵, and hence it avoids several of the similitude problems associated with
11 the use of the linear elastic ΔK parameter. This would make it extremely useful as a
12 growth rate characterising parameter, if a reliable DIC technique was developed that
13 was also demonstrated to give an appropriate value for plastic CTOD. At present,
14 various assumptions are made regarding the position behind the crack tip where this
15 should be measured.
16
17
18
19
20
21
22

23 Using the slip-based blunting mechanism at the crack tip proposed by Laird and Smith⁹
24 and Pelloux¹⁰, McClintock¹¹ showed that crack growth advance could be related to
25 $\Delta CTOD$. A sharp crack extends through alternating shear and therefore becomes
26 blunted. Crack propagation and striation formation on the fracture surface were caused
27 by the successive blunting and re-sharpening originated at the crack tip during each
28 loading cycle. Nicholls¹² explored the crack blunting concept and found for different
29 alloys a polynomial relationship between crack opening and crack advance. Donahue
30 et al.¹³ reported that da/dN and COD could be related for many different materials by a
31 constant of proportionality and the threshold stress intensity factor. Shahani et al.¹⁴
32 proposed two potential relationships to relate da/dN to $\Delta CTOD$ and ΔJ where the
33 constants remained unchanged with respect to stress ratio changes. Fatigue tests were
34 conducted on steel compact tension (CT) specimens at constant loading amplitude and
35 stress ratio values between 0.33 and 0.6.
36
37
38
39
40
41
42
43

44 Fatigue crack growth rate has been also numerically modelled using CTOD as the
45 characterising parameter. Gu and Ritchie¹⁵ used a geometric crack tip blunting CTOD
46 model to characterise crack advance without introducing any specific failure criterion or
47 presumed slip behaviour. Reasonable agreement between the numerical results and
48 experimental data of fatigue crack propagation rate was found for 7075-T6 aluminium
49 alloy using a linear $da/dN-\Delta CTOD$ relationship. Tvergaard¹⁶ extended the work by Gu
50 and Ritchie by continuing the cyclic loading up to 200 cycles via re-meshing at different
51 stages of the plastic deformation. It was shown that CTOD commonly underwent a
52 temporary behaviour, without crack closure during several cycles, before a constant
53 behaviour with closure effect started to gradually develop. In more recent numerical
54 studies, Antunes and co-workers^{5,17} have modelled fatigue crack propagation based on
55
56
57
58
59
60

1
2
3 the plastic component of CTOD for three different aluminium alloys: 6016-T4, 6082-T6
4 and 7050-T6. Different $da/dN-\Delta CTOD_p$ relationships independent of R -ratio were
5 found, that were polynomial¹⁷ in the case of the 6016-T4 and 6082-T6 aluminium alloys
6 and linear⁵ for 7050-T6 aluminium alloy. From this work the authors concluded that
7 CTOD could be a useful alternate parameter to ΔK in the fatigue crack growth
8 characterisation.
9
10

11
12
13 The digital image correlation (DIC) technique has been widely applied to problems in
14 experimental mechanics and analysis of structural integrity problems over the last 30
15 years^{18,19}. However, relatively few studies have considered the experimental analysis of
16 CTOD using DIC. Khor et al.²⁰ used the δ_5 method²¹ with DIC to measure the CTOD,
17 where δ_5 is the CTOD measurement from two points on the surface of the specimen
18 initially set 5 mm apart. Their work used single edge notched bend (SENB) specimens
19 of austenitic stainless steel and the results were compared with CTOD measurements
20 obtained both from the silicon replication method and clip gauge fracture toughness
21 measurements. The measured CTOD value therefore did not correspond to that
22 originally defined by Wells⁸ as the opening at the tip of a crack.
23
24
25
26
27
28

29 Recently, Samadian et al.²² have proposed a novel method for the CTOD
30 measurement over the entire crack front by measuring three-dimensional profile of the
31 notched surface with 3D DIC. This method was verified by measurements of silicone
32 replicas in addition to the analysis by the finite element method. There are only a small
33 number of other studies (to the authors knowledge) that have been reported in the
34 literature. Ktari et al.²³ investigated fatigue crack propagation of AISI 4130 forged steel
35 at loading ratios of 0.1 and 0.7. They proposed a 2D DIC approach based on $\Delta CTOD$
36 to characterise fatigue crack growth and concluded that $\Delta CTOD$ could be a viable
37 characterising parameter for fatigue crack propagation. They measured $\Delta CTOD$ using
38 two virtual displacement gauges that formed an extensometer positioned at various
39 distances behind the crack tip, and obtained the value of $\Delta CTOD$ by extrapolating the
40 results to $a = 0$.
41
42
43
44
45
46
47
48

49 The authors of the present work² have recently used 2D DIC measurements of CTOD
50 to characterise fatigue crack growth in commercially pure titanium. The results of this
51 work showed that the plastic component of CTOD could be directly linked with plastic
52 crack tip deformation during crack propagation leading to the conclusion that $\Delta CTOD_p$
53 was a suitable parameter to characterise fatigue crack propagation. A linear
54 relationship independent of stress ratio was obtained between da/dN and $\Delta CTOD_p$
55 ($da/dN = 0.2706 \Delta CTOD_p$). That work was intended as a preliminary study to determine
56 whether DIC techniques could be applied with sufficient accuracy to measure sub-
57
58
59
60

1
2
3 micron CTOD displacements, as some previous work²⁴ had questioned whether DIC
4 was adequate to obtain conclusive data. A commercially pure titanium alloy was
5 chosen for this preliminary study since previous work²⁵⁻²⁷ had shown that the
6 microstructure of this material is highly amenable to the use of DIC techniques and to
7 subsequent analysis and interpretation of the data.
8
9

10
11 Examples of such work include estimating both the size and shape of the crack tip
12 plastic zone under constant²⁵ and variable²⁶ amplitude loadings, as well as calculation
13 of the stress intensity factors defined by the CJP crack tip field model²⁸ that more
14 accurately characterise the mechanisms driving a growing fatigue crack²⁷. The current
15 work extends this preliminary work to the more microstructurally complex aluminium
16 alloys (2024-T3 and 7050-T6) of interest in aerospace and transport applications.
17 Fatigue tests at *R*-ratios of 0.1, 0.3 and 0.5 were conducted on each alloy using CT
18 specimens 1 mm thick and 20 mm in width (*W*). The work used the methodology
19 proposed in² to locate the crack tip and to perform a sensitivity analysis to establish the
20 position of the two points located behind the crack tip for the accurate CTOD
21 measurement. The authors believe that this sensitivity analysis process unambiguously
22 identifies the appropriate position behind the crack tip to measure CTOD and avoids
23 inaccuracies arising from the use of approximate solutions.
24
25
26
27
28
29
30
31
32

33 **2. Material and experimental methods**

34
35 Table 1 presents mechanical property data for the AA2024-T3 and AA7050-T6 alloys
36 obtained from tensile tests. All CT specimens had dimensions in accordance with
37 ASTM E647²⁹ as shown in Figure 1. Fatigue tests at stress ratio values of 0.1, 0.3 and
38 0.5 used a maximum load of 600 N.
39
40

41
42 The experimental set-up used to conduct the fatigue tests and perform data acquisition
43 is shown in Figure 2a. A random black speckle (shown in Figure 2b) was sprayed with
44 an airbrush over a white background on one surface of each specimen for DIC
45 measurements. Fatigue tests used a 25 kN servohydraulic machine (MTS 370.02) and
46 a load frequency of 10 Hz. For the 2D DIC, a CCD camera (AVT Stingray F-504 B/C)
47 was placed perpendicularly to the specimen surface, increasing the spatial resolution
48 around the crack tip by focusing with a zoom lens (MLH-10X EO). The camera system
49 was arranged to visualise the crack propagation at the centre of the image (as seen in
50 Figure 2b), with a resolution of 8.8 $\mu\text{m}/\text{pixel}$ (field of view of 14.1 x 10.6 mm). A fibre
51 optic light source (Fiber-Lite DC-950) was used to illuminate the speckled surface of
52 the specimen and to assist better observation of the speckle pattern and improved
53 image processing.
54
55
56
57
58
59
60

1
2
3 The quality of DIC measurements is intimately related to the quality of the speckle
4 pattern existing or applied on the specimen surface. Depending on the area of the
5 specimen surface and the resolution required, the speckle pattern can be either coarse
6 or fine. In our specimen with a width of 20 mm a very fine speckle pattern was
7 necessary to obtain accurate and consistent results. An airbrush was used to spray a
8 very fine black speckle over the specimen surface and, while it is fine uniform, the
9 speckle size is also varied and rather difficult to accurately quantify.

10
11 A sequence of images for DIC analysis was captured at increments of 20 N between
12 P_{min} (60 N) and P_{max} (600 N). Hence 28 images were obtained and plotted on both the
13 loading and unloading half-cycles when CTOD data was being acquired.

14
15 Image processing was performed using the Vic-2D program³⁰ from Correlated
16 Solutions using 25 pixels as the subset size and a step value of 1 pixel to obtain the
17 maximum resolution for the displacement maps. Figure 3 shows an example of the
18 displacement fields obtained for the 7050 aluminium alloy for a load of 600 N and a
19 9.13 mm crack.

20 21 22 23 24 25 26 27 28 29 **3. Crack tip location**

30 Since the CTOD was originally defined as the opening at the crack tip⁸, a particularly
31 important aspect in its measurement is ensuring accurate location of the crack tip, as
32 this assumed location will have a strong influence in the consistency of the results.
33 Hence the methodology outlined by the authors in a previous work for locating the
34 crack tip² was applied. CTOD measurement was found from the vertical displacement
35 maps by selecting a pair of points behind the crack tip to measure the relative
36 displacement between the crack faces. The x and y coordinates of the crack tip were
37 obtained as follows. Firstly, the y -coordinate is found as the intersection point observed
38 when a set of vertical displacement profiles, plotted perpendicularly to the crack path,
39 cross the crack plane. This convergent behaviour of the profiles at a point on the crack
40 plane can be clearly seen in Figure 4a. In the example shown in Figure 4a, the range in
41 the x -direction of the plotted profiles is between 710 and 740 pixels since it had been
42 previously established as the potential location of the crack tip. The vertical
43 displacement value (0.188 mm) corresponding to this intersection point is also shown
44 in Figure 4a because it is used to locate the crack tip in the x -direction (Figure 4b).

45
46
47
48
49
50
51
52
53
54
55
56
57
58
59
60 Figure 4b plots a vertical displacement profile in the x -direction parallel to the crack
direction and allows identification of the x -coordinate of the crack tip as that point on
the displacement profile that has the same value for the vertical displacement ($v =$
0.188 mm) identified for the y -coordinate of the crack tip. The crack tip x and y

1
2
3 coordinates identified from this procedure were 722 and 623 pixels, respectively, taking
4 the upper left corner of the vertical displacement map (Figure 3b) as the coordinate
5 origin. This methodology was then applied for all the crack lengths measured during
6 the fatigue testing.
7
8
9

10 **4. Influence on CTOD measurement of the located position behind the crack tip**

11
12 The location of the two points behind the crack tip used to measure the CTOD is a
13 critical aspect in the interpretation of CTOD data and its subsequent application to
14 fatigue crack propagation. For this reason, a sensitivity study was used to explore how
15 the x and y positions can influence the CTOD value. As shown in Figure 5, two
16 distances behind the crack tip are used to define the CTOD measurement position, one
17 parallel with the crack direction (defined as L_x) and other one perpendicular to the crack
18 plane (defined as L_y).
19
20
21
22
23

24 The sensitivity study analysed the variation of the CTOD values obtained at maximum
25 load and that correspond with a range of values for one of the measurement position
26 distances, whilst keeping the other one fixed. Figure 6a shows the variation in CTOD
27 profiles as a function of the L_x measurement distance for values of L_y from 1 pixel (8.8
28 μm) to 20 pixels (176 μm). As expected, in all cases there is a stable increase in CTOD
29 values as the L_x distance increases. However, an interesting observation is that the
30 displacement profiles as a function of L_y converge to a point once $L_y > 15$ pixels (= 132
31 μm), and this point corresponds to a value of L_x of 14 pixels (= 123.2 μm). This
32 behaviour is shown in greater detail in Figure 6b, where only displacement profiles for
33 values of $L_y > 15$ pixels (132 μm) have been plotted. This magnifies the region around
34 the intersection point (marked with a square). Similar behaviour is also observed in
35 Figure 6c, where displacement profiles are plotted as a function of the L_y measurement
36 distance for a range of L_x between 1 pixel (8.8 μm) and 20 pixels (176 μm). It can be
37 observed that with L_x values ≥ 14 pixels (= 123.2 μm) the CTOD profile reaches a
38 constant value at a L_y distance of 15 pixels (= 132 μm). The constant value region is
39 marked with the yellow rectangle in Figure 6c. This analysis indicates that the CTOD
40 can be uniquely and precisely measured using data obtained from two points located
41 behind the crack tip with L_x distance of 14 pixels (123.2 μm) and L_y distance of 15
42 pixels (132 μm). All CTOD measurements were therefore using these values of $L_x =$
43 123.2 μm and $L_y = 132 \mu\text{m}$.
44
45
46
47
48
49
50
51
52
53
54
55

56 It is noted that selection of the measurement point based on the variation of CTOD at
57 maximum load is a debatable criterion and it has been suggested that the sensitivity
58 analysis could instead be done using the variation in plastic CTOD. However, the
59
60

1
2
3 graphs in Figure 6, corresponding to the sensitivity analysis, show the variation in
4 CTOD values along the directions parallel (L_x) with, and perpendicular (L_y) to, the crack
5 path and are directly obtained as the relative displacement between crack flanks. In
6 contrast, the plastic component of CTOD is obtained from an analysis throughout a
7 complete loading cycle at a particular crack length. This requires additional data
8 treatment to identify where the elastic and plastic portions of CTOD are located, and is
9 therefore an indirect method that presents significant analytical complexity, since the
10 analysis would be necessary for each measurement made in the sensitivity analysis.
11
12
13
14
15

16 **5. Results and discussion**

17 **5.1. Experimental determination of plastic CTOD**

18
19
20
21 CTOD can be resolved into its elastic and plastic components from an analysis of a full
22 loading cycle. Figure 7 shows a typical CTOD plot for a crack 9.13 mm long in a 7050-
23 T6 aluminium specimen grown at a stress ratio of 0.1. CTOD data is plotted at loading
24 steps of 20 N throughout a complete loading cycle. The analysis of the plot shown in
25 Figure 7 allows the range of elastic and plastic CTOD to be obtained, where the
26 different behaviours observed during the load cycle are identified using upper case
27 letters. The loading part of the cycle between points *A* and *B* (60 N to 140 N) is
28 associated with crack opening. Once the crack is open, there is a linear regime
29 between points *B* and *C* (140 N and 320 N) which is attributed to the elastic response.
30 From point *C*, however, the curve becomes nonlinear to the point *D* (maximum load,
31 600 N) which is linked to plastic deformation at the crack tip. The procedure followed to
32 separate the CTOD into elastic and plastic components essentially requires
33 extrapolating the linear regime between *B* and *C* to the point of maximum load (shown
34 in Figure 7). Considering the unloading half cycle, between points *D* and *E* the CTOD
35 value linearly decreases with the same slope as that found between points *B* and *C*
36 for the loading half cycle. As the load is decreased below point *E* there is a deviation
37 from linearity due to the reversed plastic deformation.
38
39
40
41
42
43
44
45
46
47

48
49 The recommended practice in Appendix X2 of the ASTM E 647 standard²⁹, that deals
50 with the determination of opening load from compliance, forms the basis of the
51 procedure used to obtain the elastic and plastic components of CTOD. This procedure
52 determines the point where the change in the linearity from elastic behaviour occurs
53 (point *C* in Figure 7). Firstly, starting just above the point marking the opening region
54 (point *B* in Figure 7), a least squares straight line (line drawn in Figure 7) was fitted to a
55 segment of the experimental data spanning a range of 25% of the load cycle. The
56 slope of this straight line was taken to represent the slope of the part corresponding to
57
58
59
60

the elastic deformation of the loading cycle. Subsequently, segments of the load cycle spanning a range of three data points (7.4% of the cyclic load range) and that overlapped each other by one data point (3.7% of the cyclic load range) were used to fit least-squares straight lines, and the slope of each segment was determined. This procedure is schematically shown in Figure 8a. Finally, the relative error in slope for each segment, compared with the elastic opening slope, was calculated and plotted as a function of the applied load (Figure 8b). The point corresponding with a transition between elastic and plastic behaviour was defined as that load value where the relative error is > 5%.

The methodology described above to determine the elastic and plastic ranges of CTOD was used to analyse the CTOD data from all the tests. Figure 9 presents the results for the ranges of elastic and plastic CTOD obtained for both aluminium alloys as a function of crack length. The elastic range data show significant scatter, while those corresponding to the plastic CTOD range show a less scattered and gradually increasing behaviour as the crack grows.

5.2. Experimental fatigue crack growth characterisation by plastic range of CTOD

Figure 10 presents crack growth rate plots as da/dN versus total ($CTOD_t$), elastic ($CTOD_{el}$) and plastic ($CTOD_p$) CTOD values for the 2024-T3 alloy (Figure 10a) and the 7050-T6 alloy (Figure 10b). In both alloys, only the CTOD plastic range exhibits a linear increase with crack propagation rate and can therefore be used as a fatigue crack growth characterising parameter. Figure 11 shows the resulting $da/dN-\Delta CTOD_p$ relationships for both alloys and there is a clear linear relationship that is independent of stress ratio in each case. These growth rate equations are given below:

$$AA2024-T3: \quad \frac{da}{dN} = 0.4982 \Delta CTOD_p \quad (2)$$

$$AA7075-T6: \quad \frac{da}{dN} = 0.7313 \Delta CTOD_p \quad (3)$$

Several points should be noted about these relationships; firstly, they are linear rather than logarithmic, as is the case when using the Paris relationship. Secondly, both da/dN and $\Delta CTOD_p$ have units of length, and hence the slopes of the growth rate relationships in Equations (2) and (3) are dimensionless, in contrast with the constants defined by the Paris relationship. According to this, the constants in Equations (2) and (3) can be established as an intrinsic property of the material since they do not depend on stress ratio. Recently, Antunes et al.⁵ have also reported a linear variation between experimental da/dN data and numerical $\Delta CTOD_p$ data on MT specimens of 7050-T6

1
2
3 alloy. Their work combined numerical modelling of CTOD using a methodology they
4 had proposed in earlier work¹⁷, with experimental data for crack propagation rate
5 obtained at various stress ratio values. They found a different crack growth rate slope
6 of 0.5246 compared with the value of 0.7313 obtained in the present work. This
7 difference may reflect either the difference in methods (reference 5 combines
8 numerical modelling with experimental data while the present work is entirely
9 experimental) or the difference in specimen geometry. Whilst these aspects require
10 further work to understand and resolve, an important conclusion from both studies is
11 that a linear relationship exists between crack advance per cycle and the plastic range
12 of CTOD. The present work has also shown that sub-micron DIC resolution is quite
13 possible, and that there is apparently a unique CTOD measurement position that can
14 be easily located using DIC techniques.

23 6. Conclusions

24
25 Fatigue crack propagation rate in both 2024-T3 and 7050-T6 aluminium alloys has
26 been shown to be linearly related to the plastic range of CTOD. This work has
27 demonstrated that, using DIC, it is experimentally possible to measure the elastic and
28 plastic components of CTOD as the relative displacement between the crack flanks.
29 This work has further shown that DIC techniques can be successfully used to measure
30 sub-micron values of ΔCTOD_p in microstructurally complex aluminium alloys as well as
31 in more equiaxed CP titanium². A sensitivity analysis of measurement point location,
32 both horizontally behind the crack tip and vertically from the crack plane, has indicated
33 that an optimum position exists for these measurements. This location was identified
34 through a sensitivity analysis, based on the shape and change in shape of the various
35 measured CTOD profiles (Figure 6), and is believed to give an appropriate value of the
36 blunting CTOD, based on the shape and motion of the various CTOD profiles (Figure
37 6). The data in Figure 6 indicate that the CTOD value can be accurately measured
38 using two points located a distance behind the crack tip of 123.2 μm and a distance
39 perpendicular to the crack plane of 132 μm . To obtain accurate measurements of
40 CTOD the crack tip must be correctly located and this was done using the method
41 reported by the present authors in a previous paper².

42
43 It is clear that the use of CTOD as a parameter to characterise fatigue crack
44 propagation rate offers a more physically meaningful and mechanistically-based
45 interpretation of fatigue crack growth rate than is possible with the stress intensity
46 factor range defined by Paris. Since CTOD also includes effects of crack shielding,
47 residual stresses and fatigue threshold in an intrinsic way⁵ it avoids several of the
48
49
50
51
52
53
54
55
56
57
58
59
60

1
2
3 similitude problems associated with the use of the linear elastic ΔK parameter to
4 describe non-linear plasticity-based fatigue crack growth.
5

6
7 Finally, the different linear crack growth curves obtained for the two aluminium alloys,
8 characterised by $\Delta CTOD_p$ vs da/dN , indicate that the plastic range of CTOD appears to
9 be a material property that is independent of mechanical parameters in the loading but,
10 as might be expected, does reflect the alloy composition and microstructure.
11
12

13 14 **Acknowledgements**

15
16 The authors want to acknowledge the financial support from the Spanish Government
17 through the research project "Proyecto de Investigación de Excelencia del Ministerio de
18 Economía y Competitividad MAT2016-76951-1-P", without which this work could not
19 have been performed.
20
21
22
23
24
25
26
27
28
29
30
31
32
33
34
35
36
37
38
39
40
41
42
43
44
45
46
47
48
49
50
51
52
53
54
55
56
57
58
59
60

Review Copy

References

1. Williams JC and Starke EA Jr. Progress in structural materials for aerospace systems. *Acta Materiala*. 2003; 51: 5775–5799.
2. Vasco-Olmo JM, Díaz FA, Antunes FV, James MN. Characterisation of fatigue crack growth using digital image correlation measurements of plastic CTOD. *Theoretical and Applied Fracture Mechanics*. 2019; 101: 332–341.
3. Paris PC, Gomez MP, Anderson WE. A rational analytical theory of fatigue. *Trend Engineering*. 1961; 13: 9–14.
4. Paris PC, Erdogan F. A critical analysis of crack propagation laws. *Journal of Basic Engineering*. 1963; 85(4): 528–534.
5. Antunes FV, Branco R, Prates PA, Borrego L. Fatigue crack modelling based on CTOD for the 7050-T6 alloy. *Fatigue & Fracture of Engineering Materials & Structures*. 2017; 40: 1309–1320.
6. Hosseini ZS, Dadfarnia M, Somerday BP, Sofronis P, Ritchie RO. On the theoretical modelling of fatigue crack growth. *Journal of the Mechanics and Physics of Solids*. 2018; 121: 341–362.
7. Anderson TL. *Fracture Mechanics: Fundamentals and Applications*. Boca Raton, USA: CRC Press LLC; 2005.
8. Wells AA. Unstable crack propagation in metals-cleavage and fast fracture. *Proceedings of the Crack Propagation Symposium*. 1961; 1(84): Cranfield, UK.
9. Laird C, Smith GC. Crack propagation in high stress fatigue. *The Philosophical Magazine: A Journal of Theoretical Experimental and Applied Physics*. 1962; 7(77): 847–857.
10. Pelloux RMN. Crack extension by alternating shear. *Engineering Fracture Mechanics*. 1970; 1: 697–704.
11. McClintock FA. Discussion to C. Laird's paper 'the influence of metallurgical microstructure on the mechanisms of fatigue crack propagation'. In: *Fatigue Crack Propagation*, ASTM STP 415. 1967; American Society for Testing and Materials, Philadelphia, PA: 170–174.
12. Nicholls DJ. The relation between crack blunting and fatigue crack growth rates. *Fatigue & Fracture of Engineering Materials & Structures*. 1994; 17(4): 459–467.
13. Donahue RJ, Clark HM, Atanmo P, Kumble R, McEvily AJ. Crack opening displacement and the rate of fatigue crack growth. *International Journal of Fracture Mechanics*. 1972; 8(2): 209–219.

14. Shahani AR, Kashani HM, Rastegar M, Dehkordi MB. A unified model for the fatigue crack growth rate in variable stress ratio. *Fatigue & Fracture of Engineering Materials & Structures*. 2008; 32: 105–118.
15. Gu I, Ritchie RO. On the crack-tip blunting model for fatigue crack propagation in ductile materials. *ASTM Special Technical Publication*. 1999; 1332: 552–564.
16. Tvergaard V. On fatigue crack growth in ductile materials by crack-tip blunting. *Journal of the Mechanics and Physics of Solids*. 2004; 52: 2149–2166.
17. Antunes FV, Rodrigues SM, Branco R, Camas D. A numerical analysis of CTOD in constant amplitude fatigue crack growth. *Theoretical and Applied Fracture Mechanics*. 2016; 85: 45–55.
18. Chu TC, Ranson WF, Sutton MA, Peters WH. Applications of digital-image correlation technique to experimental mechanics. *Experimental Mechanics*. 1985; 25: 232–244.
19. Sutton MA, Orteu JJ, Schreier HW. *Image Correlation for Shape, Motion and Deformation Measurements: Basic Concepts, Theory and Applications*. New York, USA: Springer Science + Business Media; 2009.
20. Khor W, Moore PL, Pisarki HG, Haslett M, Brown CJ. Measurement and prediction of CTOD in austenitic stainless steel. *Fatigue & Fracture of Engineering Materials & Structures*. 2016; 39: 1433–1442.
21. Schwalbe KH. Introduction of δ_5 as an operational definition of the CTOD and its practical use. ASTM STP 1256. 1995; American Society for Testing and Materials, Philadelphia, PA: 763–778.
22. Samadian K, Hertelé S, De Waele W. Measurement of CTOD along a surface crack by means of digital image correlation. *Engineering Fracture Mechanics*. 2019; 205: 470–485.
23. Ktari A, Baccar M, Shah M, Haddar N, Ayedi HF, Rezai-Aria F. A crack propagation criterion based on Δ CTOD measured with 2D-digital image correlation technique. *Fatigue & Fracture of Engineering Materials & Structures*. 2014; 37(6): 682–694.
24. Korsunsky AM, Song X, Belnoue J, Jun T, Hofmann F, De Matos PFP, Nowell D, Dini D, Aparicio-Blanco O, Walsh MJ. Crack tip deformation fields and fatigue crack growth rates in Ti-6Al-4V. *International Journal of Fatigue*. 2009; 31(11): 1771–1779.
25. Vasco-Olmo JM, James MN, Christopher CJ, Patterson EA, Díaz FA. Assessment of crack tip plastic zone and shape and its influence on crack tip shielding. *Fatigue & Fracture of Engineering Materials & Structures*. 2016; 39: 969–981.

- 1
- 2
- 3 26. Vasco-Olmo JM, Díaz FA, James MN, Yang B. Crack tip plastic zone evolution
- 4 during an overload cycle and the contribution of plasticity-induced shielding to
- 5 crack growth rate changes. *Fatigue & Fracture of Engineering Materials &*
- 6 *Structures*. 2018; 41: 2172–2186.
- 7
- 8
- 9 27. Yang B, Vasco-Olmo JM, Díaz FA, James MN. A more rationalisation of fatigue
- 10 crack growth rate data for various specimen geometries and stress ratios using the
- 11 CJP model. *International Journal of Fatigue*. 2018; 114: 189–197.
- 12
- 13
- 14 28. Christopher CJ, James MN, Patterson EA, Tee KF. Towards a new model of crack
- 15 tip stress fields. *International Journal of Fracture*. 2007; 148: 361–371.
- 16
- 17 29. ASTM, E 647 Standard Test Method for Measurement of Fatigue Crack Growth
- 18 Rates. 2015, American Society for Testing and Materials: Philadelphia, PA.
- 19
- 20 30. <https://www.correlatedsolutions.com/vic-2d/>
- 21
- 22
- 23
- 24
- 25
- 26
- 27
- 28
- 29
- 30
- 31
- 32
- 33
- 34
- 35
- 36
- 37
- 38
- 39
- 40
- 41
- 42
- 43
- 44
- 45
- 46
- 47
- 48
- 49
- 50
- 51
- 52
- 53
- 54
- 55
- 56
- 57
- 58
- 59
- 60

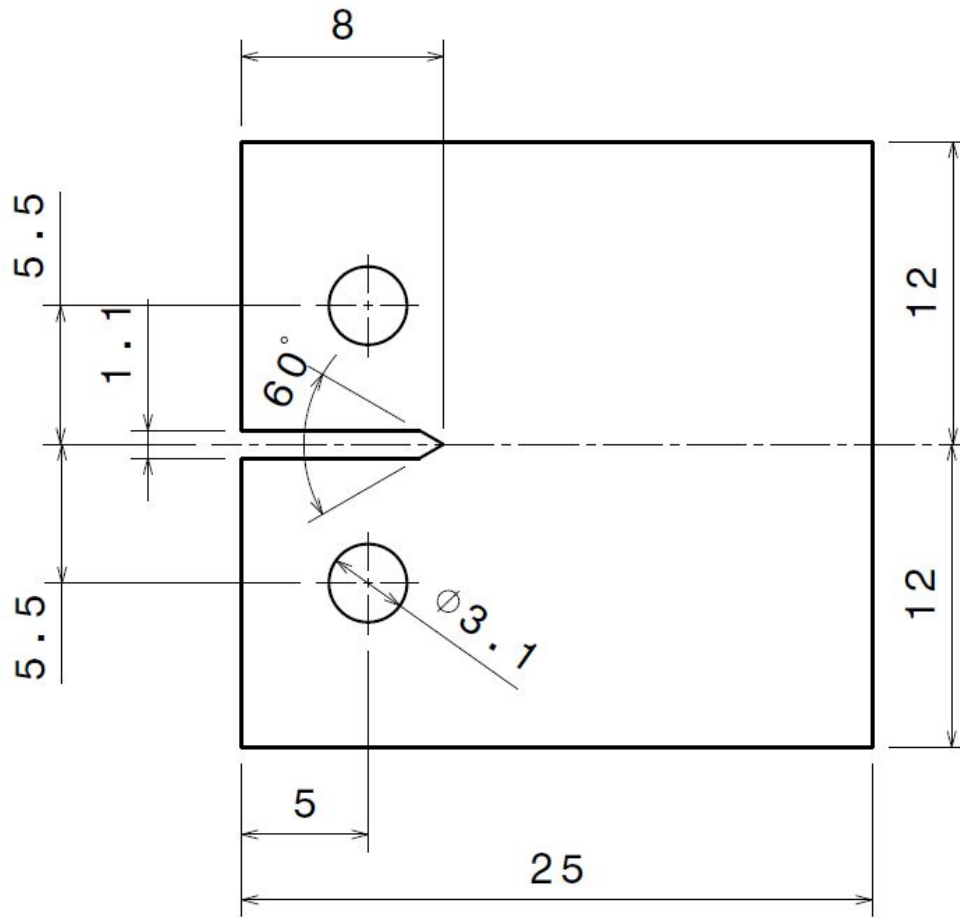
Review Copy

Table 1 Mechanical properties for the aluminium alloys analysed in the present work

Mechanical property	Unit	Aluminium Alloy	
		2024-T3	7050-T6
Young's modulus, E	GPa	72.3	71.7
Yield stress, σ_{YS}	MPa	348	546
Poisson's ratio, ν	-	0.33	0.33

Review Copy

Figures

Figure 1 Dimensions (mm) of the CT specimens²⁹.

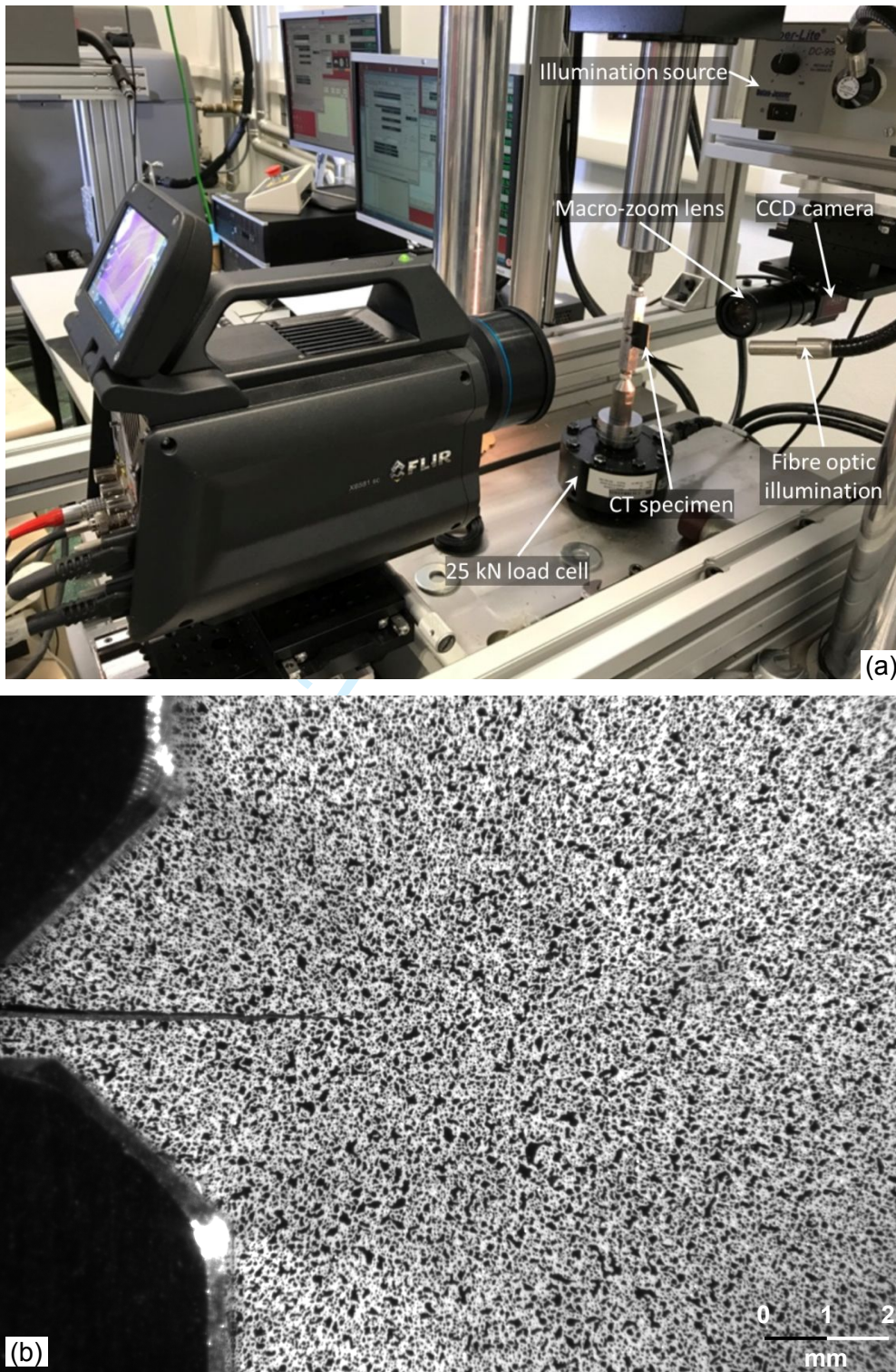


Figure 2 (a) Experimental set-up used in the paper to conduct the fatigue tests and for data acquisition. (b) Image showing the speckle pattern applied on one of the specimen surfaces to implement DIC.

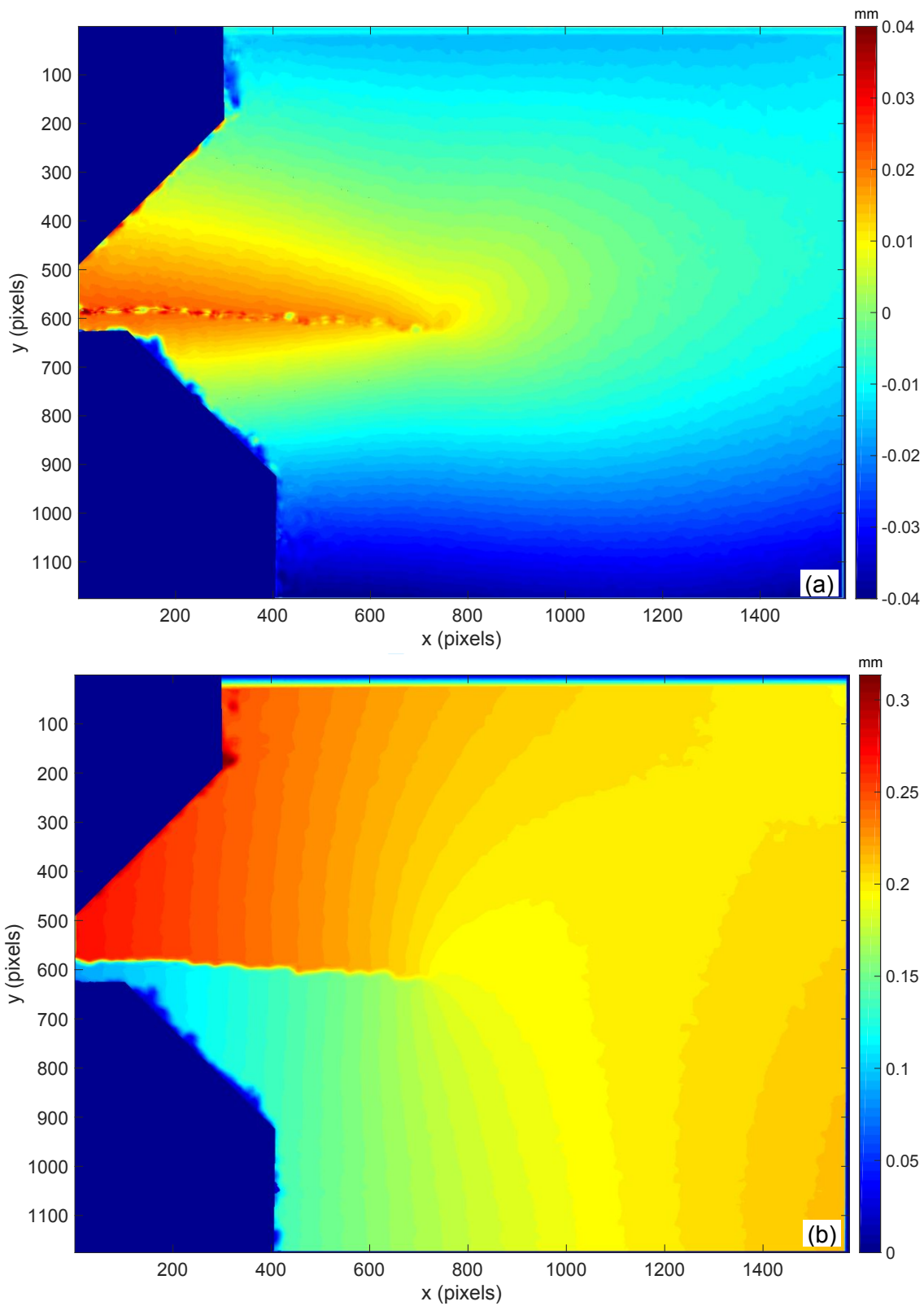


Figure 3 Example of displacement fields obtained by 2D DIC for a load of 600 N and a 9.13 mm crack: Horizontal (a) and vertical (b) displacement maps.

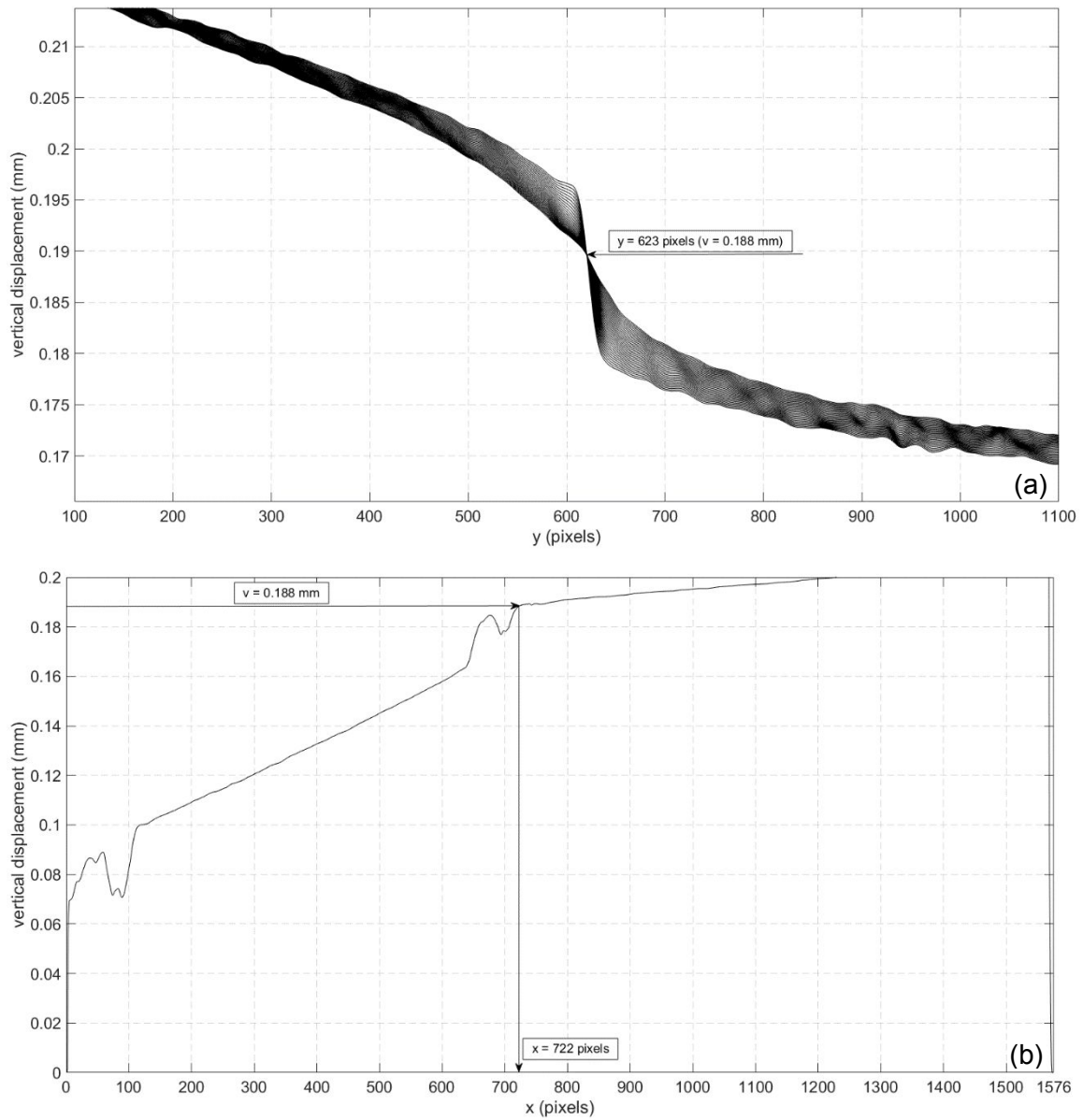


Figure 4 Plots showing the methodology used to identify the position of the crack tip in the y (a) and x (b) directions.

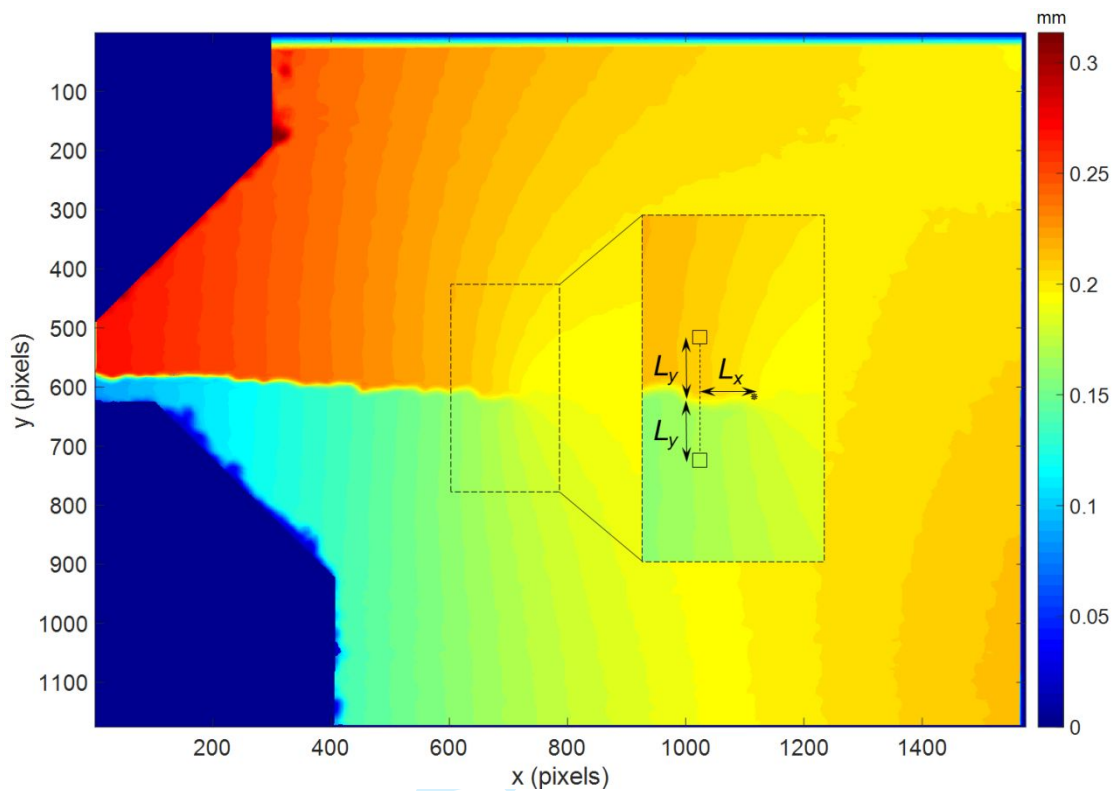


Figure 5 Vertical displacement map with the region around the crack tip enlarged to show the location of the two points used to measure the CTOD. L_x is the horizontal distance behind the crack tip and L_y is the vertical distance from the crack plane.

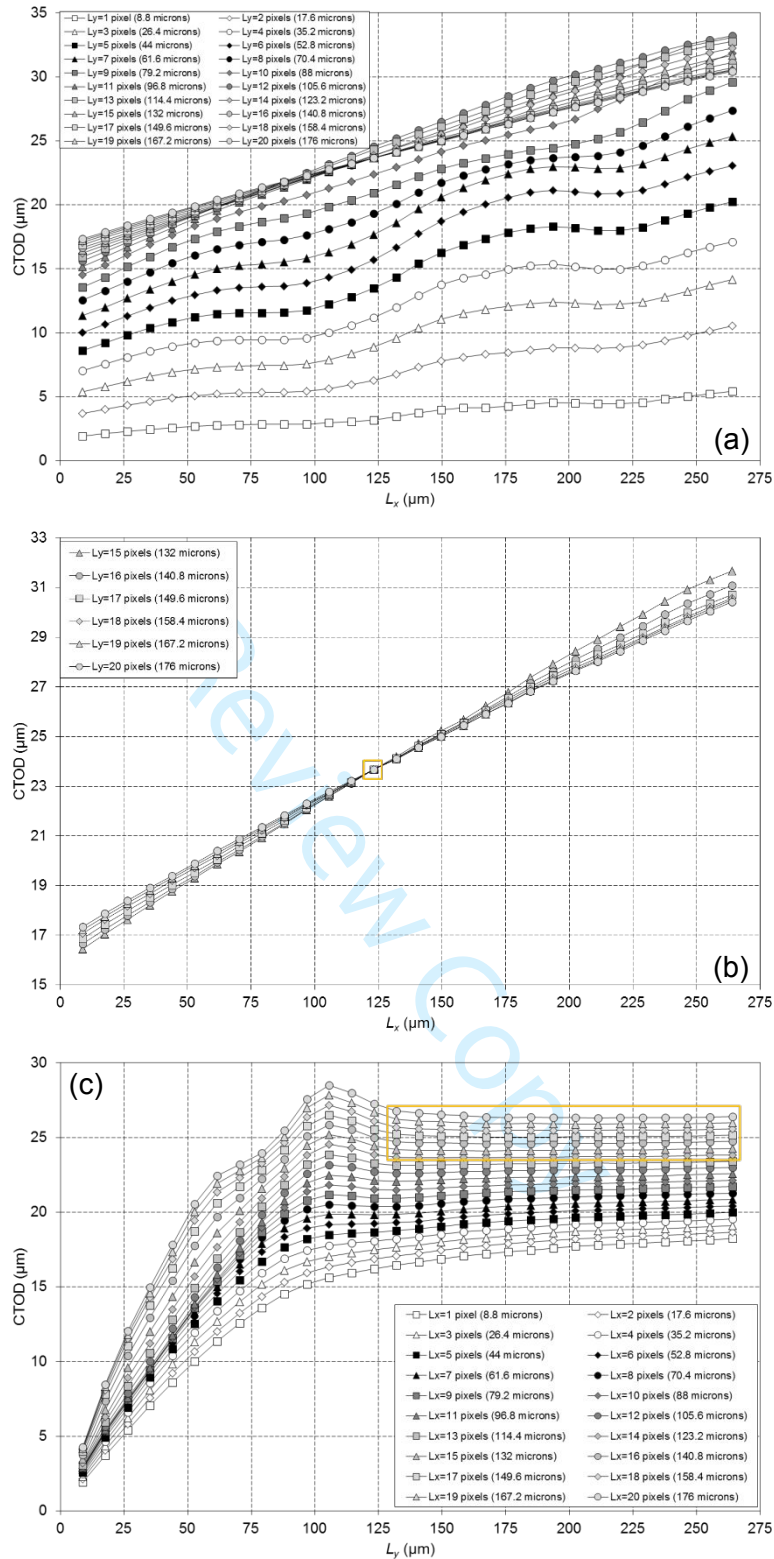


Figure 6 Plots of CTOD showing the effect of the position chosen for the two points where CTOD is measured: (a) Variation of the CTOD values with the distance L_x in the parallel direction to the crack, marking the point where the plots intersect (b); (c) Variation of the CTOD values with the distance L_y in the normal direction to the crack path.

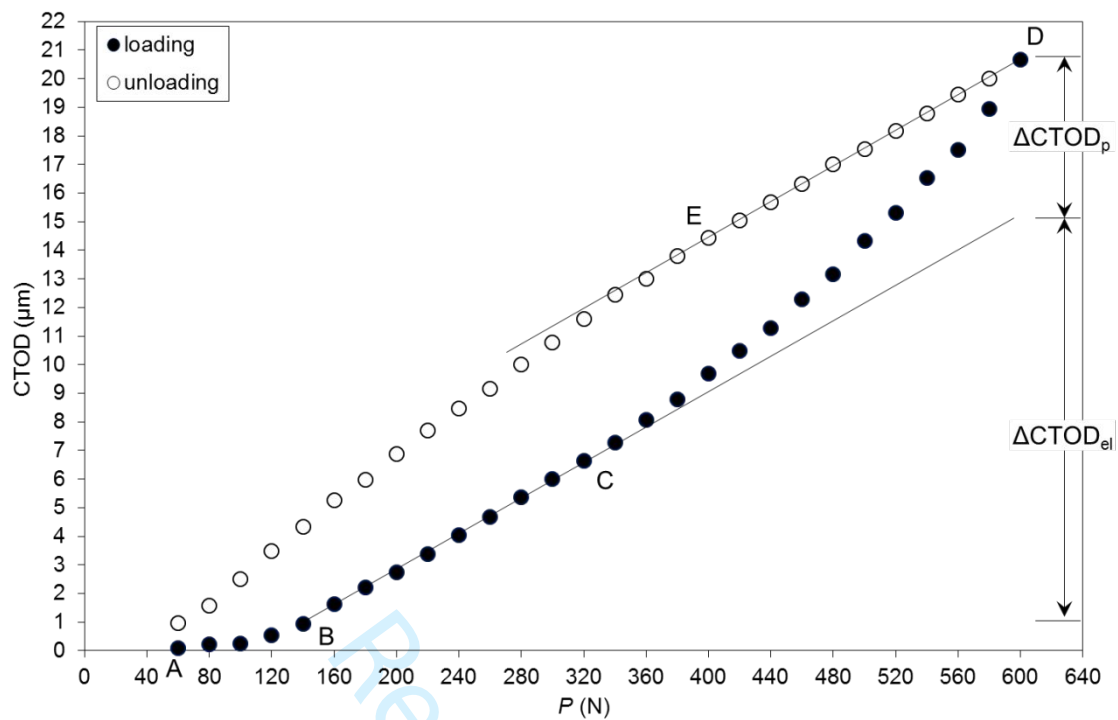


Figure 7 Variation in CTOD throughout a full load cycle for the 7050-T6 aluminium specimen analysed at $R = 0.1$ and for a 9.13 mm long crack, showing the range of its elastic and plastic components.

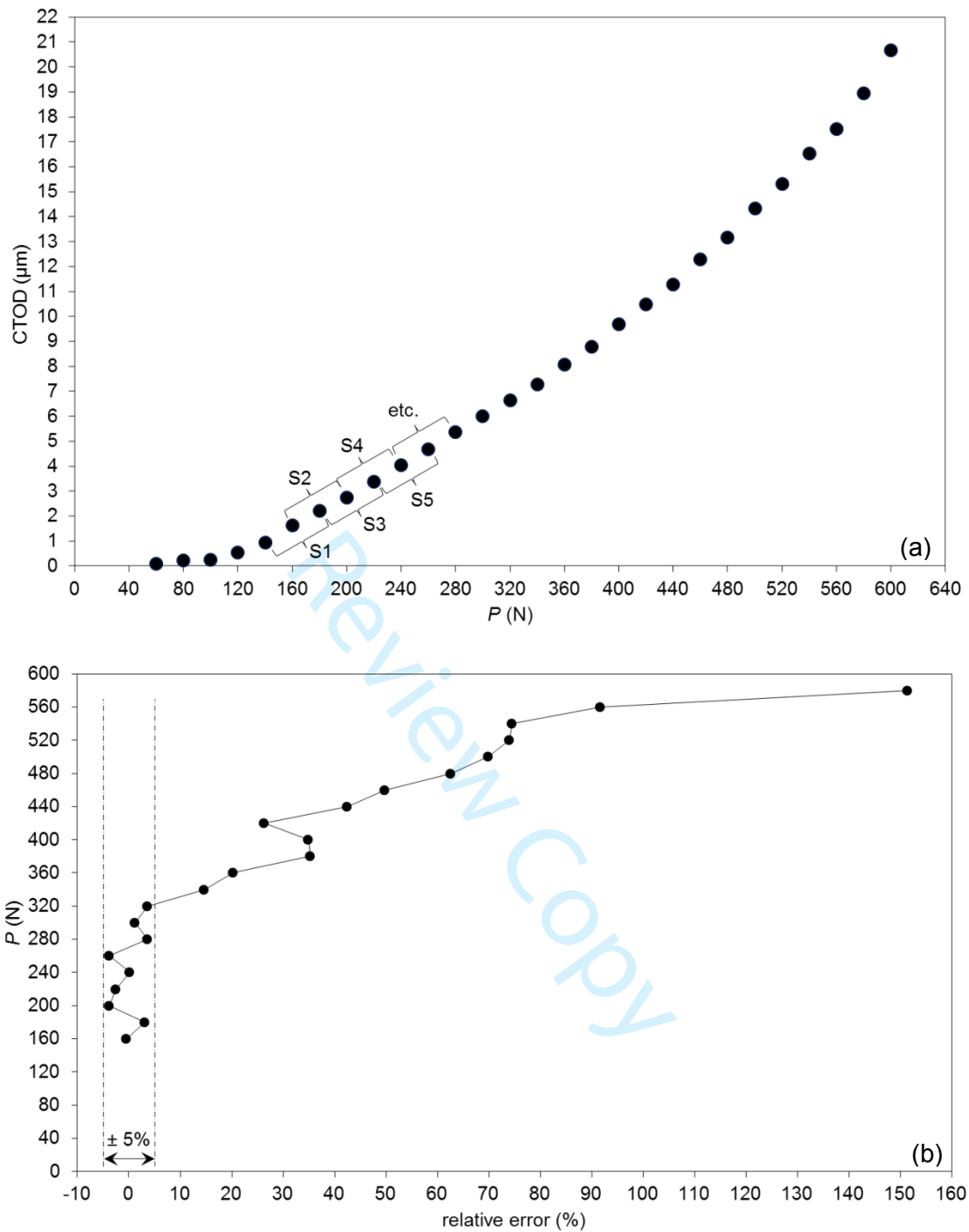


Figure 8 (a) Illustration of the technique used to analyse the CTOD data and determine the ranges of the elastic and plastic CTOD. (b) Variation of the relative error with the applied load. A change in slope of 5% was established as the criterion to identify the end of the region linked to the range of the elastic CTOD.

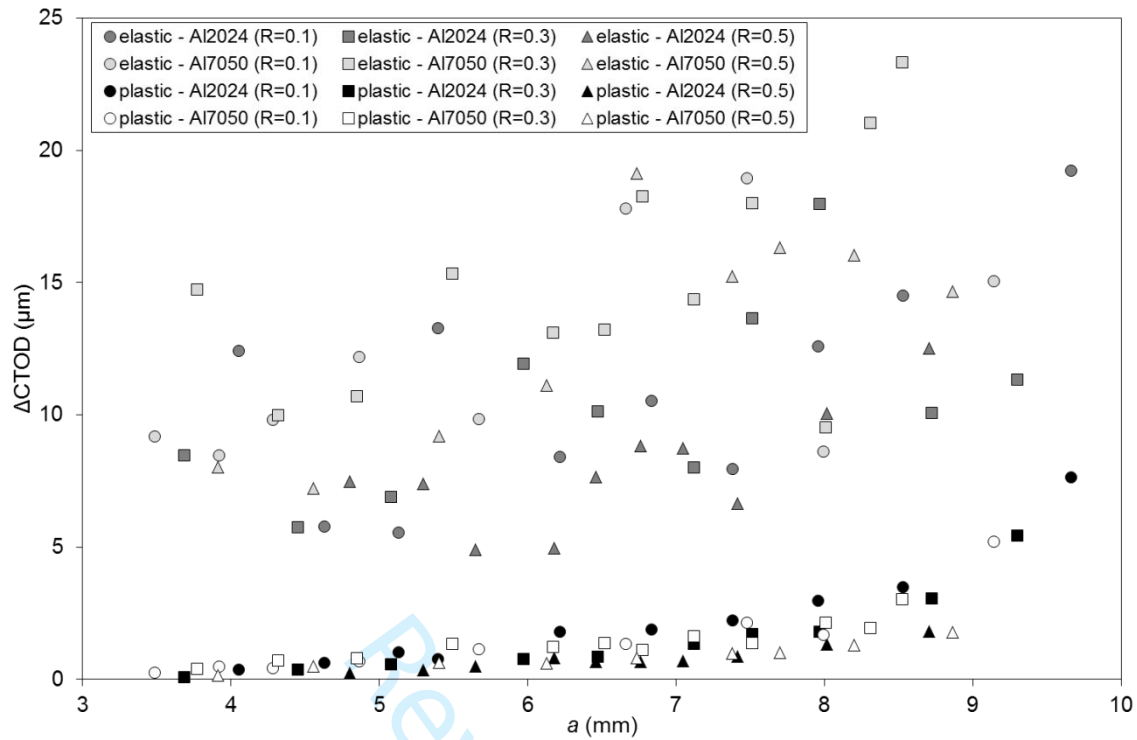


Figure 9 Ranges of elastic and plastic CTOD along the crack length at different stress ratio values for both aluminium alloys.

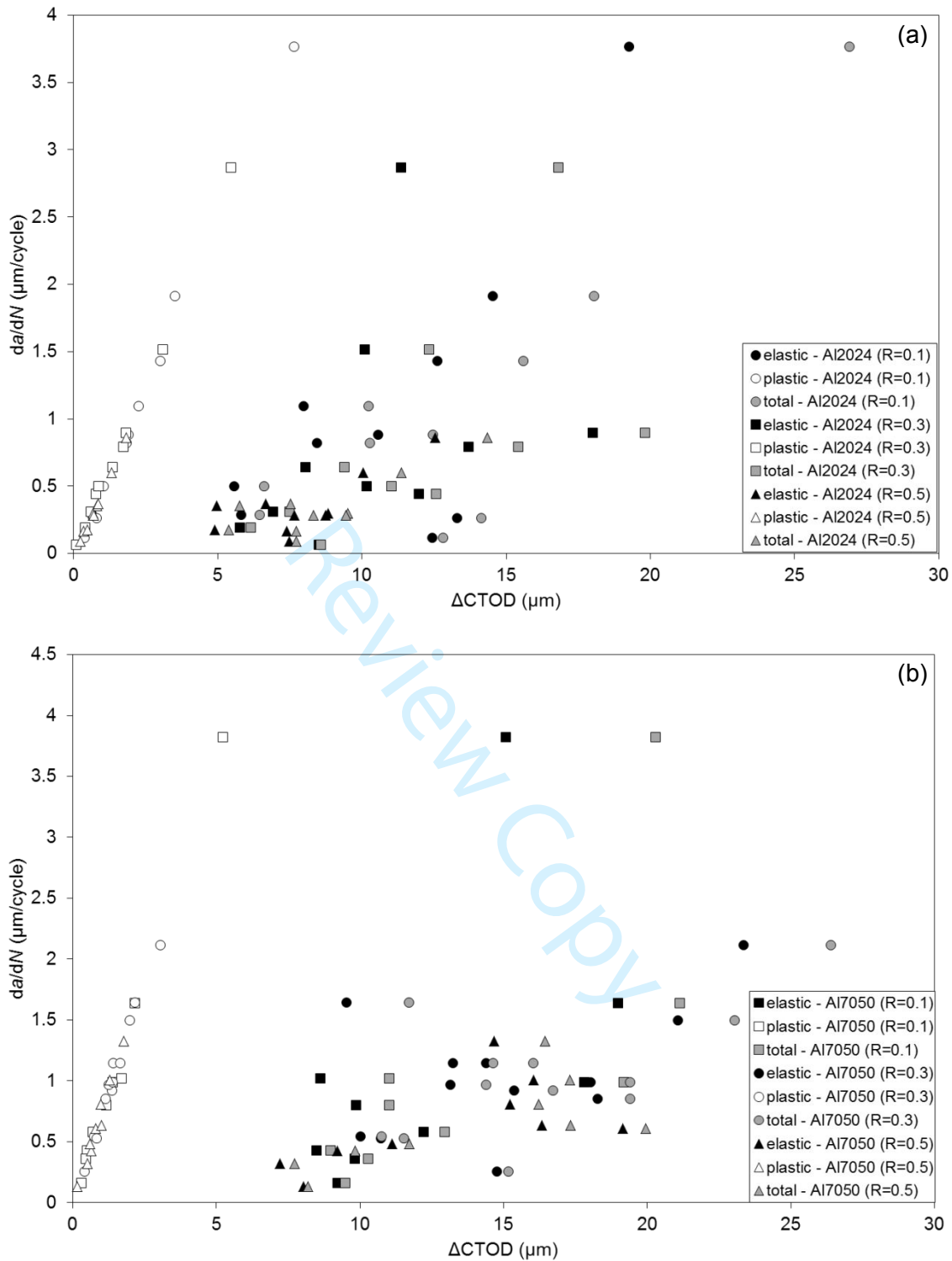


Figure 10 Plots of da/dN versus ΔCTOD corresponding to the total, elastic and plastic CTOD for the 2024-T3 (a) and 7050-T6 (b) aluminium alloys.

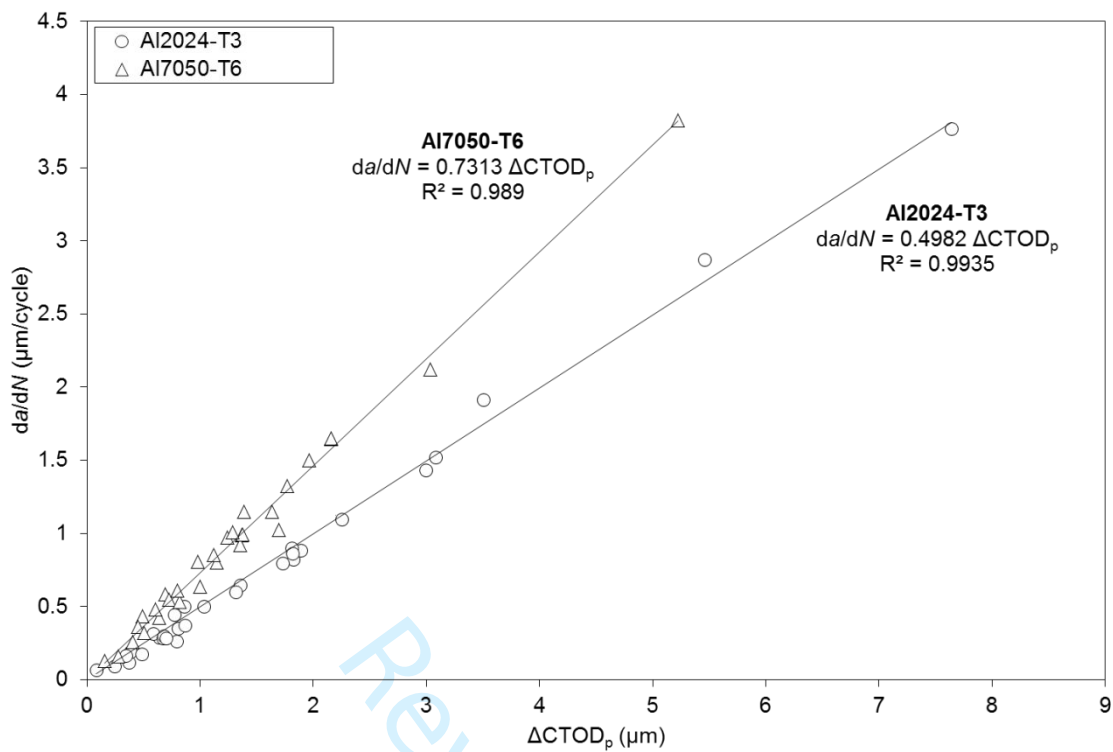


Figure 11 Graph showing the linear variation between da/dN and ΔCTOD_p obtained for both materials.